

## AN X-RAY DIFFRACTION INVESTIGATION OF AQUEOUS SYSTEMS OF DESOXYRIBONUCLEIC ACID (Na SALT)

by

D. P. RILEY AND G. OSTER\*

*The Royal Institution, 21, Albemarle Street, London (England)*

Nucleic acid is an essential constituent of living animal cells. In its desoxy variety, it constitutes the major part of the nucleus, in association or combination with protein. The exact nature of the interaction between protein and nucleic acid is not known. Chemical analyses show<sup>1</sup> that the nucleus contains about 14% by weight of desoxyribonucleic acid and in local regions the concentration may be higher. According to MIRSKY AND RIS<sup>2</sup>, 37% by weight of chromatin threads consists of nucleic acid.

The aim of this work has not been to achieve a detailed analysis of the nucleic acid molecule itself, but to study molecular arrangement in aqueous systems at relatively high concentrations. It is felt that knowledge of molecular interaction in environments similar to those which exist in the living cell may be more important to an understanding of gross cytological phenomena than even a complete picture of the molecule taken in isolation. For this type of investigation, the method of X-ray diffraction analysis is uniquely suited. It has the virtue of being indifferent to the nature of the specimen, which can be a solid, a concentrated or dilute solution, or living tissue, and of not affecting the material in the course of experiment. Linear dimensions in the 1 Å. to 100 Å. range can be accurately measured and still higher values are accessible by the low-angle scattering technique. In this paper, we shall examine the X-ray scattering given by aqueous systems of the sodium salt of desoxyribonucleic acid in concentrations varying from about 0.03 to 1.8 g/ml (2% to 100% by volume). Certain aspects of the problem have already been briefly described by us elsewhere<sup>3</sup>.

### THE MATERIAL

Three samples of the sodium salt of desoxyribose nucleic acid (from calf thymus) having different molecular weights were studied. (1) Sample prepared by Prof. R. SIGNER AND Dr H. SCHWANDER<sup>4</sup> who kindly presented it to us. This material is of very high purity and contains less than 0.3% protein. (2) Sample prepared by Drs J. A. V. BUTLER AND K. A. SMITH<sup>5</sup> who kindly presented it to us. (3) Commercial sample purchased from the British Drug Houses Ltd. Samples (1) and (2) were prepared by modifications of the Hammarsten technique (salt extraction) and sample (3) was prepared by the Feulgen-Levene technique (alkali extraction). By a comparison of the ultra-violet

\* Present address: Polytechnic Institute of Brooklyn, 99, Livingston Street, Brooklyn 2, New York, U.S.A.

absorption of solutions of these samples with the absorption for samples dried over  $P_2O_5$  and then dissolved in water (optical density of dehydrated nucleic acid at  $260\text{ m}\mu$  equals 0.200 for a solution of concentration  $1.0 \cdot 10^{-5}\text{ g/ml}$ ) it was found that the air-dry samples, as received, contained (1) 30%, (2) 30% and (3) 10% water by weight respectively. By light scattering and viscosity studies, the molecular weights (in millions) of the samples have been found to equal (1) 3.26, (2) 1.34 and (3) 0.51<sup>6</sup>, and the axial ratios 175, 125 and 19 respectively. The partial specific volume of nucleic acid is taken as 0.55, the mean of the observed values<sup>7</sup>. In all the work considered here the nucleic acids are in the form of their sodium salts.

From sedimentation and diffusion measurements extrapolated to infinite dilution<sup>7,8</sup>, the diameter of the fundamental particle, assuming it to be an elongated ellipsoid obeying the laws of macroscopic hydrodynamics, is calculated to be 18.4 Å. The rate of sedimentation for elongated particles is determined by their cross-sectional area. In the very dilute solutions required by this method, the molecules are apparently hydrodynamically independent and the dimensions thereby derived are those of the individual molecule. Electron microscope examination (with palladium shadowing) of dried solutions of SIGNER's sample shows fibres with diameters of about 50 to 60 Å.<sup>9</sup> These apparently correspond to bundles of the fundamental molecular fibres, as will be seen from the later discussion.

#### THE SPECIMENS

Specimens of known concentration were prepared from the SIGNER and from the BUTLER samples\* by the following method. Bundles of air-dry fibres were introduced into weighed thin-walled Pyrex glass tubes (average diameter 1.2 mm and wall thickness 0.04 mm). The tubes were then re-weighed and distilled water introduced with a micro-syringe; a final weighing after careful sealing-off completed the process. Specimens prepared in this way, without stirring, were left to stand for several days to attain equilibrium. This was indicated by the fact that the spacings of the X-ray diffraction bands did not change on further keeping and were the same for different parts of the specimen. On keeping for several months, however, the SIGNER specimens do show changes which are discussed later. A solution of the SIGNER sample of known concentration was also prepared by rapid stirring in a small vessel before being sucked up into the specimen tube with the aid of a vacuum pump. This specimen also showed differences from those prepared without mechanical agitation. Solutions of the commercial sample are not highly viscous and were prepared separately before being sucked into the tubes.

Work on the crystalline-micelle transition was done with the aid of a small vacuum-tight cell with thin mica windows. This cell was also used for much of the wide-angle work and for a number of exploratory experiments where the concentrations were not measured in advance.

#### X-RAY PHOTOGRAPHY

All X-ray photographs were taken with  $CuK\alpha$  radiation ( $\lambda = 1.542\text{ Å}$ ) obtained from the large rotating-anode X-ray generator in the Davy-Faraday Laboratory. Con-

\* We shall, for brevity, refer to these two samples by the names of the first mentioned authors in the references previously given<sup>4,5</sup>.

siderable modifications have been made to this unit since it was first described by MÜLLER AND CLAY<sup>10</sup>, in order to make it less troublesome to operate for prolonged periods. As the X-ray effects examined consist of relatively well-defined bands, it was not considered necessary to use crystal-reflected radiation and sufficiently monochromatic X-rays were obtained by filtering through 0.025 mm of nickel.

The camera used was essentially an optical bench mounted in a long vacuum chamber so that specimen-to-film distances of up to 110 cm could be used if needed. The beam was defined by three slits, one on the tube-window and the other two in the vacuum chamber. The latter two were precisely adjustable by micrometer screw-threads and were faced with pure tungsten. The third slit, following the usual practice, merely suppressed secondary scattering from the second slit. Little difficulty was found in obtaining by this means fine well-collimated beams of height *ca* 3 mm at the specimen.

The low-angle photographs were taken on a flat film at various distances between 15 cm and 50 cm. The wide-angle photographs were mainly taken in a cylindrical camera of radius 5 cm although some were taken at longer distances on flat film to increase the resolution. The exposure varied considerably, the wide-angle photographs requiring from 15 to 30 minutes while the low-angle exposures were of about 2 hours duration with a power input of 15 KW, the long exposures being made necessary by the great distance between the X-ray tube focus and the film. In order to eliminate air-scattering, all low-angle photographs were taken in a vacuum; this procedure was also used for most of the wide-angle work.

#### GENERAL CLASSIFICATION OF THE SYSTEMS

The structural nature of nucleic acid preparations is markedly dependent on the quantity of water present and on the way in which the sample is prepared. If insufficient water is present, or again if there is too much, the structure is disordered. There is, however, a wide range of concentrations over which the gels have an ordered structure, including a narrow range where the material appears to be really crystalline.

Four principal regions of concentrations may be distinguished and will be described in turn.

##### a. *Dry region*

This region starts at the anhydrous material ( $c = 1.0$ )\* and includes the air-dry fibres as received ( $c = 0.57$  or  $1.04$  g/ml). The anhydrous material, prepared by drying out a wet gel in a vacuum chamber containing  $P_2O_5$ , is hard, white and opaque.

##### b. *Crystalline region*

Crystalline samples, in which the concentration is in the neighbourhood of 0.44 (weight concentration, 80%) can be prepared in the following way. A drop of distilled water is added to a small amount of the air-dry fibrous substance (*ex* SIGNER). The material rapidly imbibes water and loses its opacity and shape. A homogeneous solution is obtained by stirring with a needle and this is left to dry gradually for about 24 hours. The crystalline substance which results is a hard mass with a white waxy appearance. It is opaque in bulk but shows under low magnification strong domain birefringence in

\* All concentrations  $c$ , unless stated otherwise, are given in terms of the volume of anhydrous material per unit total volume.

References p. 546.

thin sections, the domains being elongated in shape and negatively birefringent. Once obtained, the material can be wetted and dried between narrow limits without losing its essential crystalline nature.

### c. *Micelle region*

Over a wide range of volume concentrations, from about 0.4 to 0.02 (73% to 4% wt/vol), the nucleic acid gels possess a partly-ordered structure of the "liquid-crystalline" type. The striking feature of this region is that the molecules aggregate into micelles; the distance apart of molecules within micelles, as of the micelles themselves, increases markedly with dilution. These characteristics will be fully discussed in a later section. The appearance of the samples varies from that of a moist semi-opaque fibrous mass to that of a typical transparent liquid gel of high viscosity. The more concentrated transparent samples exhibit pronounced domain birefringence under static conditions, the domains being in some cases as large as 0.1 mm in length, as well as strong streaming birefringence.

### d. *Dilute region*

At concentrations less than about 0.02, the systems are transparent non-birefringent solutions of relatively low viscosity. There is no evidence of marked molecular ordering or aggregation in this region.

## GENERAL DESCRIPTION OF THE X-RAY SCATTERING

Previous X-ray work on nucleic acid preparations by ASTBURY AND BELL<sup>11</sup> and ASTBURY<sup>12</sup>, has been of a fundamentally different type from ours and has been aimed at elucidating the intramolecular structure. Fibre photographs obtained by these workers of stretched films in air showed marked preferred orientation. A list of spacings is not given but the presence of a strong meridian arc of spacing 3.34 Å. is emphasised: the true identity spacing along the fibre axis is stated to be at least 27 Å. In his latest paper, ASTBURY<sup>12</sup> states that the true repeat distance along the fibre axis corresponds to the thickness of 8 or 16 nucleotides. The principal side-spacing reported has a value of 16.2 Å. and higher spacings up to about 26 Å. are also mentioned. It may not be possible to compare these data with our findings in detail as the material used was not identical and the specimens were prepared in different ways. We shall return to ASTBURY's work in the discussion at the end of the paper.

As will be seen by reference to Table I, the X-ray scattering effects observed by us from the samples examined can be grouped into eight ranges\*. First of all, there are the 3 Å., 4 Å. and 5 Å. ranges which are given under all conditions and must correspond to intramolecular periodicities. (They were not looked for in the most dilute systems owing to the confusing effect of scattering by the bulk of water present). In the anhydrous specimen, they take the form of very diffuse bands, as they do in the case of a wet gel. The air-dry fibres (BUTLER, as received) show a significant difference in that the 3 Å. band becomes a sharp line of spacing 3.25 Å., although the rest of the pattern remains diffuse. The crystalline specimens show only sharp lines, several in each region, and the diffuse bands in the disordered structures correspond to a blurred-out

\* This statement refers specifically to the SIGNER AND BUTLER samples. Specimens made from the commercial material were examined for high spacings only.

TABLE I  
SUMMARY OF X-RAY RESULTS FOR NUCLEIC ACID UNDER VARIOUS CONDITIONS,  
SHOWING THE RELATION OF THE PRINCIPAL DIFFRACTION REGIONS TO THE DIFFERENT STRUCTURE TYPES

Specimen	Anhydrous	Air-dry fibres as received	Crystalline	Moist Crystalline	Wet gel	Wet gel
Volume Concentration	1.0	0.57	0.44	0.40	0.15	ca 0.15
Spacing Range						
3 A	3.31 <i>s vb</i>	3.25 <i>s sb</i>	2.97 <i>w</i> 3.15 <i>m</i> 3.34 <i>w</i> 3.50 <i>w</i>	a)	(a)	3.32 <i>s b</i>
4 A	4.04 <i>s vb</i>	4.14 <i>vw vb</i>	3.88 <i>m</i> 4.04 <i>s</i> 4.20 <i>m</i>	(a)	(a)	4.13 <i>vw b</i>
5 A	5.30 <i>mw b</i>	5.46 <i>vw vb</i>	4.53 <i>w</i> 4.66 <i>w</i> 5.23 <i>mw</i> 5.88 <i>w</i>	(a)		5.73 <i>w b</i>
8 A	(b)	(b)	6.54 <i>w</i> 7.22 <i>w</i> 7.97 <i>w</i>	6.67 <i>w</i> 7.33 <i>vw</i> 8.14 <i>w</i>		8.56 <i>w b</i>
10 A			10.4 <i>s</i> 11.2 <i>m</i>	10.8 <i>mw</i> 11.7 <i>m sb</i>		
15 A			15.7 <i>mw sb</i>	14.9 <i>mw</i> 16.5 <i>m</i> 19.1 <i>w sb</i>	13.2 <i>vw vb</i>	13.0 <i>m b</i>
20 A	(c)			20.8 <i>vs sb</i>	21.2 <i>vw b</i> 35.8 <i>vs b</i>	(d)
Micelle Band 40 A	(a)	(a)	(a)	44.9 <i>vw b</i>	78.5 <i>ms b</i>	(a)
(1)	(2)	(3)	(4)	(5)	(6)	(7)
						(8)

*vs* = very strong; *s* = strong; *ms* = medium strong;

*m* = medium; *mw* = medium weak; *vw* = very weak;

*vb* = very broad; *b* = broad; *sb* = slightly broadened line.

a. This spacing range not recorded

b. Weak unlocalized scattering

Spacings are in Å., concentrations in ml/ml.

The intensities given are relative intensities for any one specimen and are not directly comparable with those for another.

c. Intense diffuse central scattering

d. Intense low-angle scattering unresolved owing to small camera radius.

N.B. The columns are numbered at the base of the table.

version of the richer crystalline pattern. There is not necessarily an exact equivalence in spacing between the strongest crystalline lines and the diffuse bands but they are all obviously related to an intramolecular structure which remains substantially unaltered on this scale under all the conditions studied. The 8 Å. region is also given at all concentrations but is much less definite and intense. It, too, is probably largely intramolecular in nature.

Scattering is not observed in the remaining four spacing-ranges (10 Å., 15 Å., 20 Å., and 40 Å. upwards) in the case of material from the dry region, if exception be made for the usual diffuse central (low-angle) blackening given by disordered colloidal substances. This also applies to dilute solutions, which give diffuse central scattering only.

Specimens in the crystalline and micelle region, however, show pronounced diffraction effects in the higher spacing ranges which have been the subject of special study. Broadly, the lines in the 10 Å. and 15 Å. ranges are characteristic of a crystalline specimen, while the bands in the 20 Å. and 40 Å. ranges correspond to micelle formation. Several series of photographs were taken to establish the nature of the transition, a given slightly moist specimen being repeatedly examined as it slowly dried.

A typical wet gel in the micelle region shows two bands at low angles whose spacings are markedly dependent on the concentration of nucleic acid in the specimen. The exact way in which these bands move with concentration will be the subject of the next section. Such a system may, if it is not too dilute, also show diffuse bands in the 3 Å., 4 Å., 5 Å. and 8 Å. ranges and, in addition, one at about 13 Å. At the high concentration end of the region, lines typical of the crystalline state appear, first very faint and rather diffuse, then more and more definite as crystallisation sets in. Correspondingly, the micelle bands become fainter until they disappear, the band of higher spacing vanishing considerably ahead of the 20 Å. band. The crystalline lines, once apparent, do not change appreciably in spacing or relative intensity. They consist of a triplet of lines of spacings 10.6 Å., 11.3 Å. and 11.8 Å. and a doublet whose components are at 14.9 Å. and 16.5 Å. Under conditions of poor resolution, the two sets of lines appear as two bands of spacings 10.9 Å. and 15.7 Å. The latter composite band can be still further broadened at concentrations where the 20 Å. micelle band is just appearing. Nevertheless, there is clear evidence from several photographs that the micelle band is a separate phenomenon and is not, as a rapid inspection of one or two patterns might misleadingly indicate, the 16 Å. crystalline band shifted inwards. The transition from the crystalline state to a micelle system is reversible and a given specimen can be repeatedly changed, back and forth, from one to the other by adjusting the water-content.

The micelle band has not been observed with a spacing of less than 19.1 Å. When its spacing has this value, the band is weak whereas the crystalline line-pattern is well developed. We may therefore take this figure as the lower limit of movement of the band. If the concentration of nucleic acid is then slightly increased by allowing specimen to dry a little, the micelle band disappears completely and the crystalline pattern only is seen.

#### THE X-RAY PHOTOGRAPHS

We have reproduced in Fig. 1, 2, and 3 a selection of X-ray photographs given by nucleic acid under various conditions.

Fig. 1 reproduces four wide-angle photographs taken in order to show the lower

*References p. 546.*

spacing regions in specimens of different moistness. Photographs Ia, b, c were taken in a cylindrical camera of 5 cm radius, while Id was taken on flat film at 5.5 cm distance.

1a. A photograph of the crystalline material, showing a wealth of well-defined lines reminiscent of the patterns given by normal crystalline substances in powder form. The spacings and relative intensities are listed in Table I, column 4. The substance was enclosed in the small air-tight cell described earlier.

1b. A similar photograph of the same crystalline specimen in a slightly more moist state. Note the blurring of the lines which otherwise remain practically unchanged. The specimen was enclosed in a cell, as in 1a.

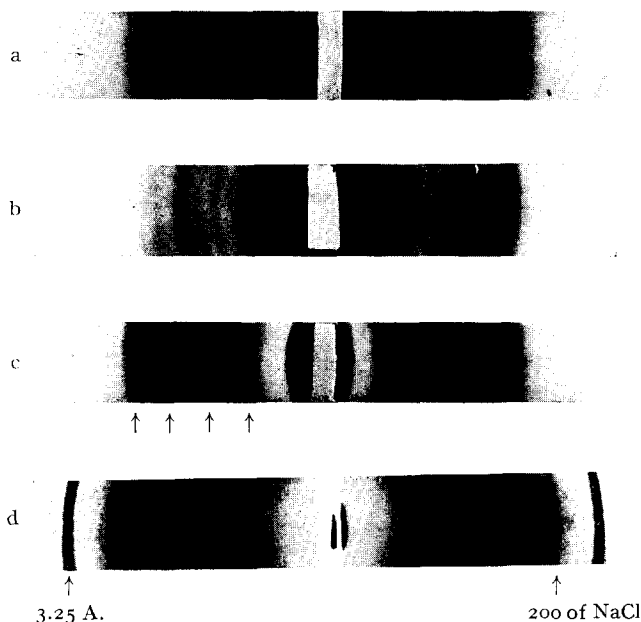


Fig. 1. Wide-angle photographs of various specimens of nucleic acid (CuK $\alpha$  radiation, Ni filter).

- a. Crystalline specimen in cylindrical camera of 5 cm radius
- b. Moistened crystalline specimen in same camera
- c. Anhydrous (P<sub>2</sub>O<sub>5</sub> dried) specimen in same camera
- d. Bundle of air-dry fibres, as received, at 5.5 cm on flat film.

1c. The pattern given by anhydrous material obtained by prolonged drying of a gel in a vacuum over P<sub>2</sub>O<sub>5</sub>. Details of the photograph are given in Table I, column 2. The photograph was taken in a vacuum camera with the specimen unsurrounded by any enclosure.

1d. A photograph of a bundle of air-dry fibres (BUTLER AND SMITH, as received). Details are given in Table I, column 3. The dominant feature is a sharp line of spacing 3.25 Å. and the 200 line of NaCl present in the sample is also shown.

Fig. 2. Shows a series of photographs taken to illustrate the gradual transition from the crystalline state to the micelle region. All photographs were taken on flat film in a vacuum camera, 2a at 20 cm, the rest at 15 cm.

2a is a photograph of a crystalline specimen corresponding to the central higher-

spacing region of Fig. 1a. The triplet and doublet, the spacings of which are given in Table I, column 5, are clearly resolved (*T* and *D*). There is no evidence of other crystalline lines of high spacing but the micelle band  $M_1$  is just starting to be perceptible at its lowest observed spacing of 19 Å.

2b shows how, on addition of a tiny amount of water,  $M_1$  becomes more pronounced and slightly increases its spacing (Table I, column 6). The crystalline lines are still present.

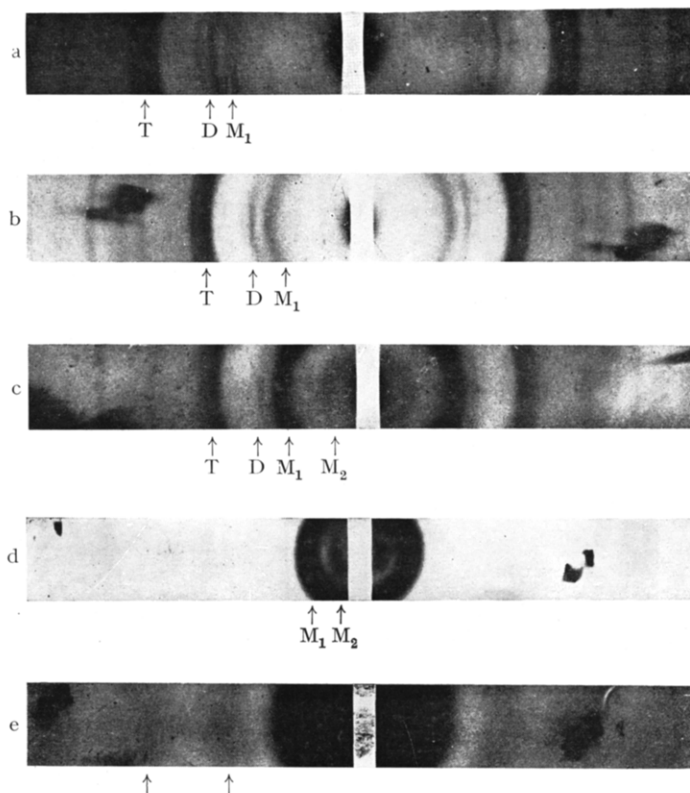


Fig. 2. Photographs to show the transition from the crystalline state to the micelle region. CuK $\alpha$  radiation, Ni filter, in a vacuum camera. (a) at 20 cm on flat film (b) (c) (d) and (e) at 15 cm on flat film. (d) and (e) are under- and over-exposed prints of the same photograph. Micelle bands are shown by  $M_1$  and  $M_2$ , crystalline doublets and triplets are labelled *D* and *T*. Arrows in (e) indicate diffuse low-spacing scattering regions. Concentration diminishing from (a) to (d) with consequent onset of micelle formation. Large spots are from mica-windows of specimen-cell.

2c shows the effect of further addition of water.  $M_1$  is now the dominant feature of the pattern and the inner micelle band  $M_2$  is just becoming visible. The crystalline pattern is weaker and less distinct.

2d and e are photographs of a transparent wet gel prepared from the above specimen by addition of water and stirring. 2d is a light print which shows clearly the two micelle bands, now at much higher spacings (Table I, column 7). 2e is a heavy print of the same photograph made in order to show how the perfection of the crystalline pattern has been lost and replaced by the broad scattering regions indicated by arrows.



Fig. 3 reproduces low-angle photographs given by the three different samples of nucleic acid investigated. All were taken in a vacuum camera, 3a at 30 cm, the other two at 25 cm, with the specimens enclosed in thin-walled glass tubes.

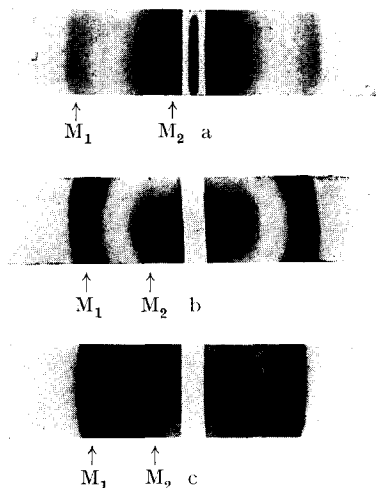


Fig. 3. Low-angle photographs showing differences in micelle bands given by three samples of nucleic acid.

a. SIGNER AND SCHWANDER, fresh and unstirred. Volume concentration 0.182 (33% wt/vol); b. BUTLER AND SMITH. Volume concentration 0.250 (45% wt/vol); c. Commercial (BDH). Volume concentration 0.274 (50% wt/vol)  $\text{CuK}\alpha$  radiation, Ni filter, in vacuum camera. (a) at 30 cm (b) and (c) at 25 cm.

inner band shifting more rapidly than the outer. The sharpness and intensity of the bands also change with concentration.

As will be seen from Table II and Fig. 3, the SIGNER and SCHWANDER material gives photographs which are distinctly different from those given by the other two samples. The inner band  $M_2$  is similar in definition and intensity to the outer band  $M_1$  and, in the three more dilute specimens, is actually the stronger of the two. The commercial sample resembles that of BUTLER AND SMITH in that the outer band  $M_1$  is always stronger and usually sharper than the inner,  $M_2$ . In all cases, dilution tends to broaden both  $M_1$  and  $M_2$ . In the most dilute systems  $M_2$  is no longer observed, and the region between  $M_1$  and the central beam is filled in with a nearly uniform background. The more concentrated specimens prepared from the BUTLER material, and from the commercial sample, give an outer band  $M_1$  which is unsymmetrical. Although quite sharp, it possesses a visible tail on the higher-spacing side; this effect is not so apparent with freshly-prepared SIGNER specimens. Despite these minor differences, the spacings corresponding to  $M_1$  do not depend to any appreciable degree on the nature of the sample but only on the concentration of the specimen. The nature of the inner band  $M_2$  is on the contrary greatly affected by both factors. Its spacing relative to concentration is considerably higher for the SIGNER sample than for the other two, and its intensity and definition are also more pronounced.

References p. 546.

3a is a photograph of an unstirred SIGNER specimen of volume concentration 0.182. The inner band  $M_2$  is markedly more intense than  $M_1$ .

3b is a similar photograph of a BUTLER specimen of volume concentration 0.250. The print has been over-exposed to bring up the weak and broad  $M_2$  band. In the original, the outer band  $M_2$  is sharper than appears here.

3c is a similar photograph of a commercial specimen of volume concentration 0.257. The inner band is markedly weaker and more diffuse than the outer.

#### THE MICELLE REGION

All three samples of nucleic acid give pronounced low-angle diffraction effects if the concentration is between certain limits and, although there are differences in detail, the general nature of the scattering is the same in each case. It consists of two well-separated bands of which the outermost, of lower spacing, is usually the sharper and more intense. The spacings of both bands increase as the systems are diluted but at different rates, the

TABLE II  
DESCRIPTION OF THE LOW-ANGLE BANDS GIVEN BY MICELLAR SYSTEMS OF VARIOUS CONCENTRATIONS  
PREPARED FROM THREE DIFFERENT SAMPLES OF NUCLEIC ACID

Sample	Specimen	Volume Concentration $c$	Spacings in Å.			Relative Intensities	Sharpness		Other Features
			Band $M_1$ $d_1$	Band $M_2$ $d_2$	Ratio $d_2/d_1$		Band $M_1$	Band $M_2$	
SIGNER AND SCHWANDER	1	0.351	21.0	77	3.67	$I_1 = 2I_2$	Quite sharp, symm.	Quite sharp, symm.	
	2a	0.236	27.0	102	3.78	$I_1 = I_2$	Quite sharp, symm.	Quite sharp, symm.	
	b		26.0	62	2.38				
	3	0.182	30.5	116	3.80	$I_1 = 20I_2$	Sharp, unsymm.	Very broad	
	4	0.099	42.5	160	3.77	$I_2 = 4I_1$	Quite broad	Quite broad	
	5	0.067	53.0	187	3.53	$I_2 = 6I_1$	Broad	Broad	
	6	0.032	73			$I_2 = 10I_1$	Broad	Very broad	Background
	7	0.028	(65, 82) 93 (80, 112)				Very broad	Not distinguishable	Strong background
BUTLER AND SMITH	1	0.362	22.0	49	2.23	$I_1 = 10I_2$	Quite sharp, symm.	Very broad	
	2	0.250	26.0	(42, 58) 58	2.23	$I_1 = 10I_2$	Sharp, unsymm.	Very broad	
	3	0.243	27.5	(48, 73) 64	2.32	$I_1 = 10I_2$	Sharp, unsymm.,	Very broad	
	4	0.131	39.0	(55, 77) 90	2.30	$I_1 = 5I_2$	Very broad	Very broad	Background
	5	0.069	50.5 (45, 57)	{ 118 }	2.34	$I_1 = 2I_2$	Very broad	Very broad	Strong background
Commercial (BDH)	1	0.257	28.0	70	2.50	$I_1 = 6I_2$	Sharp, unsymm.	Very broad but well defined	Background
	2	0.235	29	(50, 103) { 115 }		$I_1 = 2I_2$	Broad, unsymm.	Very broad	Background
	3	0.193	34	{ 115 }		$I_1 = I_2$	Very broad	Very broad	Background
	4	0.226 (10% NaCl)	30	{ 115 }		$I_2 = 4I_1$	Very broad	Very broad	Background

\* Spacings in round brackets give the rough limits of the band. Curly brackets indicate that the value given is very approximate.  $d_1$ ,  $I_1$  and  $d_2$ ,  $I_2$  refer to the bands  $M_1$  and  $M_2$  respectively. Relative intensities are very approximate.

In three cases, the specimens were re-photographed after being kept untouched at room temperature for several weeks in their original sealed capillary tubes. The BUTLER samples (2 and 3) showed no significant differences after 8 weeks, whereas the SIGNER specimen (2) after 16 weeks gave a substantially altered photograph (see Table II). Whereas originally the inner band  $M_1$  was about equal in intensity and sharpness to  $M_2$ , on keeping it had become much weaker and more diffuse. The spacing of  $M_1$  had only slightly changed but that of  $M_2$  was considerably lower than at first. In short, the diffraction effects were similar to those given by BUTLER AND SMITH specimens of about the same concentration.

The characteristics of the inner band are also dependent on the way in which a specimen is prepared. In general, the specimens were prepared without the use of any mechanical agitation, equilibrium being reached in a sealed tube merely by keeping for 2 to 3 days. If, however, gels of the SIGNER sample be made up by stirring in small containers and, when visibly homogeneous, sealed up in the usual tubes or in the vacuum-tight cell, the inner band is again weaker, more diffuse and of lower spacing. A typical specimen of this type gave spacings of 45 Å. and 98 Å. for  $M_1$  and  $M_2$ ; the ratio  $d_2/d_1 = 2.15$  is substantially lower than in the unstirred specimens and resembles those found with the BUTLER samples.

One other isolated experiment needs to be mentioned. In an attempt to see whether any very weak bands were escaping observation, a very over-exposed photograph was taken of a weak gel (stirred-up SIGNER sample). The result is reported in Table I, column 7, and it will be seen that a third very weak band was present. The concentration of the specimen can be roughly gauged from the spacing of  $M_1$  (35.8 Å.) and is 0.15. The ratio of the spacing of  $M_1$  to that of the new band is 1.69. There is a rough correspondence to the ratio,  $\sqrt{3}$ , of the spacings of the 10 and 11 planes in a two-dimensional hexagonal array.

#### STRUCTURE OF THE MICELLAR SYSTEMS

In the discussion which follows, it will be taken that BRAGG's law holds for the spacings of the low-angle bands. We have elsewhere<sup>13,14</sup> given theoretical arguments in favour of this supposition in certain cases. In the nucleic acid systems, the fact that strongly birefringent domains are visible in transparent specimens under static conditions argues a high degree of crystallinity and strengthens the BRAGG law assumption.

In order to illustrate the way in which the spacings  $d_1$  and  $d_2$  of the bands depend on concentration, the relevant data of Table II have been plotted on a double logarithmic scale (Fig. 4). The main features of the graph are

- a. the points corresponding to  $d_1$  all lie on or near the same straight line (C), no matter which sample is considered or how the specimen was prepared
- b. the points corresponding to  $d_2$  lie on one of two straight lines (A or B) according to the source of the nucleic acid sample and the method of preparation of the specimen
- c. all three lines are parallel and have a slope of  $-1/2$ .

This value for the slope of the plots means that in each series the spacings are inversely proportional to the square root of the concentration. The expansion on dilution is therefore two-dimensional in each case and consequently neither spacing can relate to a simple repeat distance along the molecular axis.

The observation that  $d_1$  is dependent only on the concentration of the specimen

and not, or only slightly, on the source of the nucleic acid or the way in which the specimen is made up, suggests that it is related to some fundamental dimension in the molecule itself. All three samples, when made up into specimens of the same concentration, will give approximately the same value for  $d_1$ . The most probable explanation of these facts is that  $d_1$  is simply related to the distance of separation  $s$  of neighbouring molecules and therefore to the molecular diameter  $\sigma$ .

The larger spacing  $d_2$  derives from a further periodicity which is also subject to expansion in two dimensions. It is much more marked in the SIGNER specimens (when unstirred and fresh) than in the others. The SIGNER specimens clearly have a relatively very ordered structure. The larger periodicity is less perfect in the other specimens, and

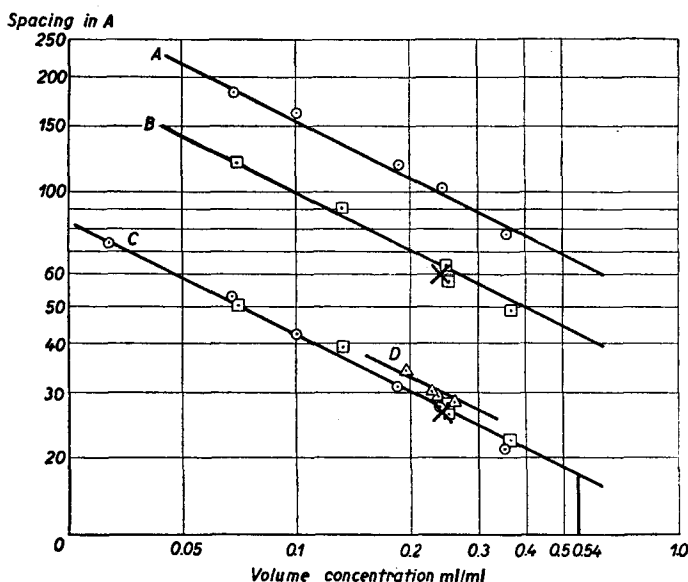


Fig. 4. Plots of the spacings  $d$  of the two micelle bands against concentration on a double logarithmic scale.

- SIGNER AND SCHWANDER specimens (fresh and unstirred) ( $d_2$  on line A,  $d_1$  on line C)
- BUTLER AND SMITH specimens ( $d_2$  on line B,  $d_1$  on line C)
- △ Commercial (BDH) specimens ( $d_1$  on line D)
- × SIGNER AND SCHWANDER specimen, after several months.

its mean value is lower. It is probably related to the micelle diameter  $\delta$  but other hypotheses will first be discussed.

At first sight, the two spacings  $d_1$  and  $d_2$  might derive from two separate phases and to two different nucleic acid molecules. With complex macromolecules, this duality is not an impossibility but the hypothesis can be excluded by a simple argument. Both spacings are observed to be proportional to  $1/\sqrt{c}$  where  $c$  is the measured concentration of the whole system. In any two phase system, each spacing would vary as  $1/\sqrt{c}$  only if  $c$  were expressed as the concentration in the phase concerned. It follows that the variation of the two spacings must be different aspects of one phenomenon. The expansion of  $d_2$  must be a consequence of the increase in  $d_1$  on dilution and not a separate effect. Only two hypotheses meet the situation. One is that of micelle formation, and the other, of regular molecular folding.

The expansion of  $d_1$  is, in the first case, intramolecular while that of  $d_2$  is inter-molecular. The micelles consist of regular bundles of long rod-like molecules and are themselves arranged in a semi-regular 2-dimensional pattern. On addition of water the constituent molecules of the micelles move further apart and hence the micelles swell laterally. As a result of this intramolecular swelling, the centre-to-centre distance between neighbouring micelles shows a corresponding increase.  $d_1$  and  $d_2$  would thus always be in the same proportion at any stage of dilution, as observed experimentally.

The second hypothesis is that the long molecules are regularly coiled or folded in such a way that two-dimensional intramolecular swelling can take place as between different longitudinal sections. As a result, the overall lateral dimensions of the molecule increase and give rise to an increase in the intermolecular spacing  $d_2$ . The scheme is best

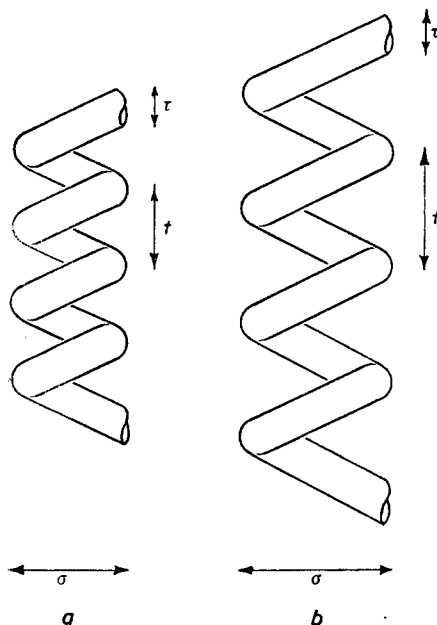


Fig. 5. Schematic picture of helical molecule at two stages of uncoiling on dilution.  $\tau$ , true molecular (fibre) diameter;  $\sigma$ , effective molecular (helix) diameter;  $t$ , repeat distance along long axis of helix.

exemplified by a regular cylindrical helix. Suppose the molecules in a concentrated specimen to be as in Fig. 5a. The longitudinal axis of the molecular chain (pictured as having a circular cross-section) is coiled into a regular helical form and there is an intramolecular periodicity  $d_1$  corresponding to  $t$ , the distance between one coil and the next. The effective diameter of the molecule is not  $\tau$ , the diameter of the chain, but  $\sigma$ , the diameter of the helix. There is therefore a further intermolecular periodicity  $d_2$  corresponding to the distance of separation  $s$  of neighbouring helices in a regularly packed two-dimensional assembly. In order that the intramolecular swelling be two-dimensional, it is necessary that the diameter of the helix  $\sigma$  expand as well as the repeat distance along its axis  $t$ . The diametral expansion of  $\sigma$  causes a corresponding increase in  $s$ , and therefore in  $d_2$  (Fig. 5b). This postulated intramolecular swelling is the equivalent of uncoiling the helix in a certain way. It is difficult to give an exact treatment of the dependence of  $d_1$  and  $d_2$  on concentration in such a case, as the various parameters defining the helix are unknown. In short, the helical

hypothesis is a very flexible one, but, because of that, is difficult to use numerically. It is, in particular, difficult to employ an extrapolation procedure to derive  $\tau$  and  $\sigma$  from the values of  $d_1$  and  $d_2$  over a range of concentrations. If this type of molecular model is correct, the interesting corollary follows that the molecule really possesses two diameters,  $\tau$  and  $\sigma$ , which might be revealed differently by different physical methods.

The alternative hypothesis of micelle formation has been subjected to detailed analysis in the case of the highly ordered SIGNER specimens. Two types of structure are possible and one may pass into the other on change of concentration. In one type, each micelle of diameter  $\delta$  is free to rotate about its longitudinal axis; in the other, neighbouring micelles register one against the other and do not rotate. In both types, the molecules are free to rotate about their long axes. That they do so rotate, or at least

oscillate, is suggested by the disappearance of the high spacing lines of the crystalline material when wetted. It seems reasonable to suppose, from the repeated wetting and drying experiments described earlier, that some components of the 10.9 Å. and 15.7 Å. composite bands are the spacings of vertical sets of planes defined by the precise location and orientation of molecules in the crystalline case. On addition of water, the molecules start to rotate and the perfection of the crystalline structure is destroyed. A paracrystalline system results in which the molecules can be approximated by cylinders of rotation and which therefore gives rise to a single intermolecular diffraction band in place of the richer crystalline line spectrum. Extrapolation of  $d_1$  to a volume concentration of unity will give a rough value for the molecular diameter. A more accurate value can only result from an extrapolation procedure which takes into account the actual structure of the micellar systems. In Fig. 4, the value of  $d_1$  extrapolated to  $c = 1$  is 13 Å. and this figure may be taken as a lower limit for  $\sigma$ , the diameter of the unhydrated molecule. Another value is given by the lowest observed value for  $d_1$ , which is *ca* 19 Å. at  $c = 0.44$ . On further drying, the band disappears altogether and the lines characteristic of the crystalline state appear. This value of  $d_1$  is presumably related to the diameter of the unhydrated molecule in a way discussed in detail below. Further, from Table II, it will be noted that at any concentration  $d_2 = 3.7 d_1$ , approximately.

A structure therefore needs to be proposed in which the micellar diameter  $\delta'$  in the hypothetical dry state, is roughly three times the molecular diameter  $\sigma$ . The micelles are probably roughly cylindrical in shape and Fig. 6 shows the obvious model to adopt. Six cylindrical molecules are

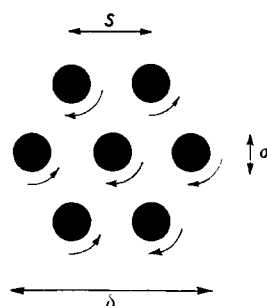


Fig. 6. Hexagonal 7-molecule micelle. Rotation of molecules indicated by arrows.  $\sigma$ , molecular diameter;  $\delta$  micelle diameter;  $s$ , distance separating centres of neighbouring molecules.

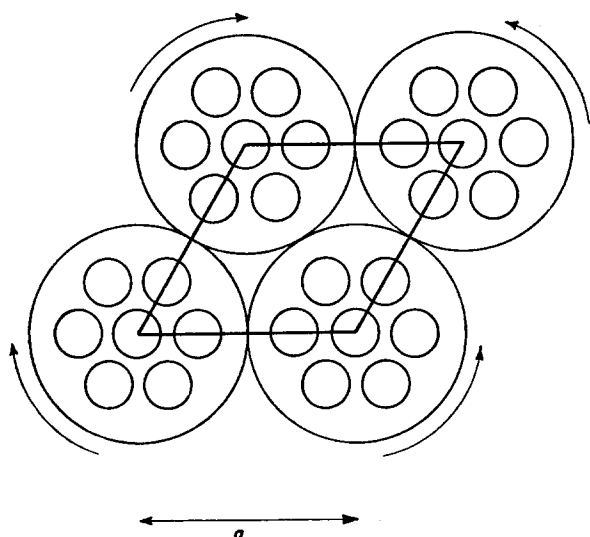


Fig. 7. Structure consisting of freely-rotating micelles in a regular hexagonal array. Rotation of micelles depicted by arrows.  $a$ , unit-cell edge.

grouped hexagonally around a central one and the whole structure expands laterally on addition of water.

The next step is to consider ways in which these 7-molecule micelles can be arranged in 2-dimensional patterns and any proposed structure must explain why  $d_2$  can be more intense than  $d_1$  in the SIGNER specimens. It must also satisfy the concentration conditions for micelle formation, as the typical bands do not appear at concentrations above about 0.44.

As mentioned above, one possibility is that the micelles are free to rotate. The depiction of this scheme in two dimensions is given in Fig. 7, which roughly reproduces the concentration conditions in the

concentrated SIGNER specimens. If the micelles are placed in a regular hexagonal 2-dimensional array, the spacing  $d_2$  would be pronounced, as it would correspond to the 10 planes of the statistical unit-cell of edge  $a$  outlined in the drawing. The spacing  $d_1$ , on the other hand, could not be crystallographic but would arise from purely intramolecular interferences. As regards  $d_1$ , the structure consists of micelles which are independent scatterers, there being no coherence between radiation scattered by one micelle and the next. The problem of evaluating the intensity of scattering by assemblies of parallel cylindrical molecules, assumed to be of infinite length, has been treated by us elsewhere<sup>14</sup>. The normalized intensity (*i.e.* per molecule) of radiation scattered by the 7-rod micelle of Fig. 5 is

$$I \propto \frac{1}{49} \left[ \frac{2 J_1(kR)}{kR} \right]^2 \left[ 7 + 24 J_0(x) + 6 J_0(2x) + 12 J_0(\sqrt{3}x) \right] \quad (1)$$

where  $J_0(z)$  and  $J_1(z)$  are the Bessel functions of order zero and unity respectively, and  $k = \frac{4\pi \sin \theta}{\lambda}$ , where  $\lambda$  is the X-ray wavelength and  $2\theta$  the scattering angle.  $x = ks = 2\gamma kR$ , where  $R = \frac{1}{2}\sigma$  is the radius of the cylindrical molecules and  $\gamma = s/\sigma$  is a factor introduced to make the expression apply to micelles of any degree of lateral dilution-expansion. Fig. 8 gives curves of  $I$  plotted against the dimensionless variable  $ks$  for two values of  $\gamma$ . It is evident that the diffraction bands are more pronounced the larger the gap between the molecules; at the same time, the maximum of the main band  $A$  moves towards a spacing corresponding to that of the 10 planes in a 2-dimensional hexagonal lattice of infinite extent. The subsidiary maximum  $B$ , which has no equivalent in the case of the infinite lattice, is a result of the small number of molecules in the micelle.

While a structure of freely-rotating micelles may apply in dilute solutions, we exclude it in the case of the concentrated systems for the following reasons:

a. the observed band  $d_1$  appears to be sharper than the band  $A$  in Fig. 8. On this hypothesis the band is most diffuse in the concentrated systems—the reverse of what is observed;

b. on dilution, the spacing of the band  $A$  decreases relative to the standard provided by the intermicellar spacing  $d_2$ . Thus, on this hypothesis, the ratio  $d_2/d_1$  would progressively increase whereas it is observed to remain sensibly constant.

We need now to consider the hypothesis that the hexagonal micelles of Fig. 6 do not rotate but are arranged in a quasi-regular 2-dimensional structure. On this basis, the problem reduces to one of solving a 2-dimensional crystal structure which is partly disordered.

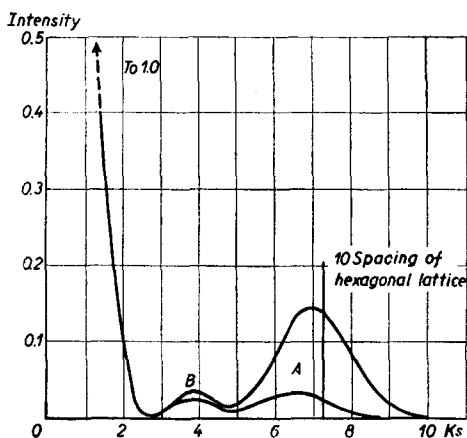


Fig. 8. Intensity curves calculated for isolated 7-molecule micelles (see Fig. 6) at two stages of dilution-expansion. Upper curve,  $s/\sigma = 2.0$ ; lower curve,  $s/\sigma = 1.25$ .

The procedure adopted was to calculate the structure amplitudes  $F_{hk}$  of the principal sets of planes  $hk$  for a large number of structural models. Micelles other than that shown in Fig. 6 were tried in this work and a variety of structural types involving them were tested.

If the system can be considered as a two-dimensional crystal, the intensity of scattering by any set of planes  $hk$  is given by

$$I_{hk} \propto f^2 |F_{hk}|^2 \quad (2)$$

where  $f$  is the molecular scattering factor for cylinders,  $2J_1(kR)/kR$ , given in equation (1). We have considered only centro-symmetrical structures, in which case  $F$  is no longer complex and may be expressed as

$$F = \sum \cos 2\pi (hx + ky) \quad (3)$$

where  $x$  and  $y$  represent the positions in the unit-cell of the different molecules, expressed as fractions of the unit-cell edges.

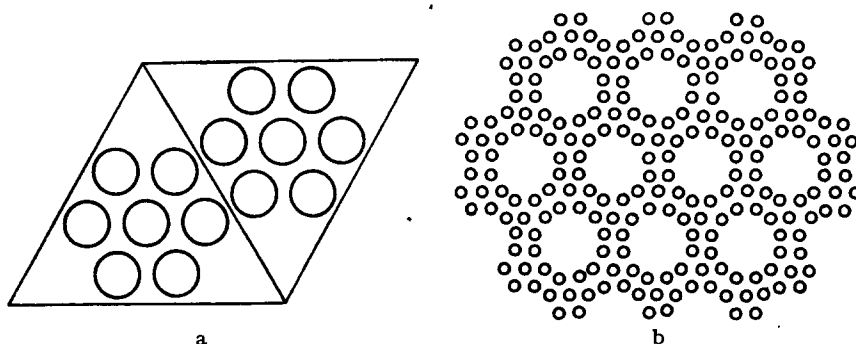


Fig. 9. Micellar structure proposed for fresh, unstirred SIGNER AND SCHWANDER specimens. (a) detail of hexagonal unit-cell containing 2 7-molecule micelles, for a concentrated specimen (b) general picture of structure showing honeycomb pattern with regularly disposed holes.

In the crystalline case, both  $d_1$  and  $d_2$  must refer to the spacings of crystallographic sets of planes or, when there is some disorder, to unresolved combinations. Owing to the rapid way in which the factor  $f^2$  diminishes with angle (*i.e.*,  $k$ ), only planes of low indices need be considered and this is obviously even more true in partly disordered structures. It is probable that the averaged overall symmetry is hexagonal, in which case simple relations exist between the interplanar spacings  $d_{hk}$  and the  $a$  dimension of the hexagonal unit-cell. From the relations it is seen that the ratio  $d_{10}/d_{31}$  is 3.61, whereas the observed ratio  $d_2/d_1$  is *ca* 3.7. The ratio  $d_{10}/d_{40}$  is, obviously, 4.0. If, as seems probable,  $d_2$  corresponds to  $d_{10}$ ,  $d_1$  must correspond to  $d_{31}$  or to an unresolved combination of  $d_{31}$  and  $d_{40}$ . It is a simple matter to derive structures in which 31 and 40 are strong reflectors. In order to make 10 strong, any proposed structure must have substantial discontinuities on the scale of the unit-cell edge  $a$ , *i.e.*, the structure must be of an open honeycomb pattern. Fig. 9 shows the structure finally adopted for which Table III gives the calculated  $F$  values for planes of low indices. For convenience in calculation, the parameters defining the positions of the molecular centres were taken to have exactly the following fractional values



$$\pm \left[ \frac{4}{9} \frac{1}{9}, \frac{2}{3} \frac{1}{9}, \frac{4}{9} \frac{1}{3}, \frac{2}{3} \frac{1}{3}, \frac{1}{9} \frac{4}{9}, \frac{1}{9} \frac{2}{9}, \frac{1}{3} \frac{4}{9} \right]$$

which makes the intermicellar gap slightly less than that between molecules within a micelle, whereas in the proposed structure, as drawn in Fig. 9, these two gaps are equal. Table III also gives the relative multiplicity factor  $p$ , *i.e.* the relative frequency of occurrence of reflecting planes related by symmetry. The theoretically estimated intensity is therefore  $pF^2$  multiplied by the appropriate value of  $f^2$  for the particular angle of reflection. As the influence of  $f^2$  will vary with the degree of dilution-expansion, we have preferred to plot  $pF^2$  only in exact form. Fig. 10 shows lines of length proportional to  $pF^2$  drawn at positions given by the reciprocal of their spacings. This method of presentation is the pictorial equivalent of an actual low-angle X-ray photograph. The smooth curve shows roughly the effect of amalgamating the broadened lines which would be the result of structural disorder, and also allows for the falling-off effect

TABLE III

GEOMETRICAL STRUCTURE FACTORS  $F_{hk}$  CALCULATED FOR THE MODEL SHOWN IN FIG. 9 WHEN ADJUSTED TO A  $\frac{1}{9}:\frac{1}{9}$  NET, TOGETHER WITH THE CORRESPONDING RELATIVE MULTIPLICITY FACTORS  $p$

$hk$	$F$	$p$	$pF^2$
10	-3.68	1	13.5
20	+0.76	1	0.6
30	+2.00	1	4.0
40	-6.08	1	37.0
11	-0.40	1	0.2
22	-2.44	1	6.0
21	+1.54	2	5.7
31	-1.88	2	7.1

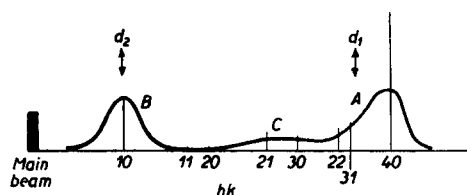


Fig. 10.  $pF^2$  values (vertical lines) for the low-order  $hk$  planes plotted against  $1/d$  for the structure drawn in Fig. 6. Smooth curve gives rough estimate of intensity distribution to be expected in a real specimen. Arrows indicate observed positions of diffraction bands.

of the  $f^2$  factor. It will be seen that the diffraction consists of the two main bands A and B connected by a region of lower intensity, the plateau C. If B corresponds to  $d_2$ , the observed mean position of  $d_1$  is shown by arrows. The position and intensity of the composite maximum A is thus in reasonable accord with experiment. Some of the SIGNER specimens do, in fact, show a slight tail on the low-angle side of the outer band as would be expected from Fig. 10 (see Fig. 3a). In the proposed structure, as stated above, the water-gap between the "contact" sides of the micelles has been taken to be the same as that between molecules within a micelle. On dilution, the whole structure expands uniformly in two dimensions and the ratio  $d_2/d_1$  remains constant. At lower concentrations, however, the structure will become progressively more disordered and the diffraction pattern correspondingly more diffuse.

This suggested structure has been derived from purely crystallographic reasoning. It remains to be seen whether it satisfies the concentration conditions observed in practice. The volume concentration of the structure drawn in Fig. 9, assuming infinitely long cylindrical molecules, is 0.54 ( $\sigma/s$ )<sup>2</sup>. At molecular contact ( $\sigma = s$ ), therefore, the volume concentration would still be quite low, 0.54. The extrapolated value of  $d_1$  at

this limiting concentration is 18 A. which compares reasonably well with the lowest observed value, 19 A., which must embrace a small water-gap.

We are now in a position to derive a figure for the unhydrated molecular diameter  $\sigma$  and to compare it with the limiting values discussed earlier. The values of the relevant interplanar spacings  $d_{hk}$  in terms of the intermolecular distances  $s$  are

$$\left. \begin{aligned} d_{10} &= 4.20 s & \dots\dots d_2 \\ d_{31} &= 1.17 s \\ d_{41} &= 1.05 s \end{aligned} \right\} \dots\dots d_1$$

As  $d_1$  is composite, it is perhaps more satisfactory to work from the  $d_2$  relation and employ the known ratio  $d_2/d_1$  to derive the factor connecting  $d_1$  and  $s$ . In this way, we find that  $d_1 = 1.14 s$ . It follows, from the extrapolated-to-dryness value of 18 A. for  $d_1$ , that the unhydrated molecular diameter  $\sigma$  is 16 A. The diameter of the dry micelle  $\delta'$  is therefore approximately 3 times this figure, which agrees with the value of *ca* 50 A. observed in the electron microscope.

The structure of the micellar systems prepared from the other two samples of nucleic acid (BUTLER AND SMITH; BDH) is less definite. Both samples give strong and sharp  $d_1$  bands whose spacings, as a function of concentration, are almost identical with those given by the SIGNER specimens. The inner  $d_2$  bands, on the other hand, are weak and very diffuse. In the case of the commercial sample, it is difficult to assign a significant mean spacing to the  $d_2$  band. The long-range order in these specimens must therefore be considerably less than that existing in the SIGNER systems.

In the case of the commercial sample, it is probable that there is only a small tendency to micelle formation. This is shown, first of all, by the extreme lack of definition of the inner band. In the most concentrated specimen,  $d_1$  is, on the contrary, very sharp and intense. This would be in accord with a simple hexagonal arrangement of molecules uniformly in two-dimensions. In such a structure, the volume concentration  $c = \frac{\pi}{2\sqrt{3}} \left(\frac{\sigma}{s}\right)^2$  and  $s$  is now given by the crystallographic relation  $\frac{2}{\sqrt{3}} d_1$  for 10 planes in a simple hexagonal array. Substitution of the known values for  $d_1$  and  $\sigma$  into these expressions ( $d_1 = 28$  A.,  $\sigma = 16$  A.) gives  $c = 0.228$ , which, when compared with the measured value of 0.257, suggests only slight micelle formation. However, a numerical argument cannot be pushed too far because of the effect of small amounts of impurity or of degraded molecules of nucleic acid which are probably present. The fact that the values for  $d_1$  for this sample lie above the others in Fig. 4 is in agreement with only slight micelle formation (line D compared with line C).

The position of the BUTLER AND SMITH specimens is intermediate. There is certainly a tendency to micelle formation as the inner band, although very broad and weak, nevertheless exists and moves rationally with change of concentration. The mean spacing of this band is considerably less than in equivalent SIGNER specimens. There is also the significant observation that SIGNER preparations, on stirring or keeping, give diffraction patterns which are practically identical with those given by the BUTLER samples. This is strong evidence that the highly organized SIGNER systems are formed only under exceptional conditions and are easily transformed into the more disordered BUTLER structures.

The essential difference between the two types would appear to be the occurrence

of large and regularly disposed water gaps in the SIGNER structures. Only by having an open honeycomb pattern as shown in Fig. 9 is it possible to make  $d_2$  sufficiently intense and well defined. It is obvious that this band will be less intense for any structure in which the molecules tend to fill space uniformly and, in the limiting case of a simple hexagonal network, it will not occur at all. In an attempt to elucidate the nature of the BUTLER specimens, we have considered possible micellar structures of intermediate density (Fig. 11). While the general trend of the  $pF^2$  plots (*cf.* Fig. 10) is in the right direction, in no single instance is it possible to arrive at close agreement with experiment. It would therefore appear that the real structure is a semi-ordered mixture of micellar structures of the sort shown in Fig. 9 and 11. An important result of the calculations is that the intense band, corresponding to the  $d_1$  spacing, does not change greatly in position under equivalent concentration conditions.

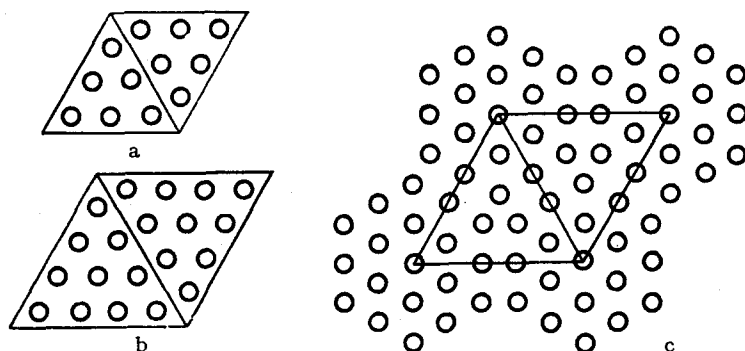


Fig. 11. Some possible micellar structures considered for the less-ordered systems.

#### GENERAL CONCLUSIONS

Our X-ray investigations have shown that desoxyribonucleic acid in solution is a system of considerable complexity. Fortunately, since the samples show relatively large crystalline domains, we are justified in applying crystallographic principles to the treatment of the data.

The nature of the variation of the two large spacings with concentration suggests immediately a two-dimensional swelling. This swelling is, however, of a higher degree of complexity than that reported for tobacco mosaic virus solutions by BERNAL AND FANKUCHEN<sup>15</sup> where the molecules simply fill space uniformly. In Fig. 9 is given a possible structural model of a nucleic acid gel which is consistent with the observed data for the sample of highest molecular-weight. The more degraded samples of nucleic acid in solution exhibit less long-range order, indicating that the proposed honeycomb structure is critically dependent on the length of the fibres. However, with all three samples studied, small local micelles of the fibrous molecules are always present except at extreme dilutions. Apparently the regular honey-comb structure is not very rigid since it can be broken down by mere mechanical agitation. This may help to explain the unusual mechanical properties of nucleic acid gels.

We cannot at the present time attempt to explain in rigorous fashion the nature of the forces acting between nucleic acid molecules in the manner applied in the case of tobacco mosaic virus<sup>16</sup>. What are lacking are thermodynamic measurements made

on concentrated solutions of nucleic acid in the presence of varying amounts of salts, in order to ascertain the role of electrostatic forces.

From consideration of the micellar systems, we arrived above at a value of 16 Å. for the diameter of the unhydrated molecule. In fact, the molecule is unlikely to be precisely cylindrical and this figure will more exactly have reference to its largest lateral dimension. It is perhaps significant that the value is close to the largest crystalline spacing of 16.5 Å. This spacing is probably the same as ASTBURY'S 16.2 Å. side-spacing and may be defined, as was suggested earlier, by the side-by-side packing of molecules along one direction. From the perfection of the diffraction pattern given by the crystalline specimen, it is clear that some hydrate of nucleic acid is formed when a critical minimum amount of water is added corresponding to a volume concentration of 0.44 (80% wt/vol). Vapour pressure measurements of this hydrate might prove instructive.

The fact that the main low-spacing diffraction regions persist, albeit sometimes blurred, in all the specimens examined, wet or dry, is strong evidence that the nucleic acid molecule is very rigid. The internal structure of the molecule must possess pronounced regularity for its principal features are still detectable in a dilute wet gel ( $c = 0.15$  or 3% wt/vol approximately) as is shown in column 8 of Table I. In a dilute sample such as this, each molecule is an independent scatterer as regards its internal periodicities in structure.

We should not like, from our data, to draw any positive conclusions regarding the detail of the internal structure of the molecule. Our results, in the main, are nevertheless not inconsistent with ASTBURY'S general picture of the nucleic acid structure. In his view, the molecule consists of a long column of flat nucleotide discs piled vertically one above another, each nucleotide having linear dimensions 15 Å.  $\times$  7.5 Å. approximately, and being joined to its neighbours through phosphoric acid links. Astbury places great emphasis on the meridional 3.34 Å. spacing he observes and assigns it to the distance separating neighbouring parallel nucleotide discs along the fibre axis. Our results, as summarised in Table I, place less emphasis on this spacing. A marked spacing at 3.25 Å. occurs in the air-dry fibres, but in the fully-ordered crystalline specimens there is no uniquely outstanding spacing in this region. There is a line actually at 3.34 Å. but there are several others, notably at 3.15 Å. and at 4.04 Å., which are as strong or stronger. Further, we have discovered no evidence of the suggested true repeat distance along the fibre axis of 27 Å. or of a still higher multiple of the 3.34 Å. spacing (16 times) as later stated by ASTBURY<sup>18</sup>. We have examined the high-spacing region carefully and have observed no diffraction lines for the crystalline material with spacings greater than 16.5 Å.

It is clear from the data presented in Table I, columns 4 and 5, that the unit-cell cannot be very large even if some of the lines are second-order reflections with the first-order absent for reasons of symmetry. Some of the lines can be tentatively indexed on the basis of an orthorhombic cell but we have not pursued the matter. Comparison of our crystalline data with ASTBURY'S should not be carried too far as his specimens were prepared in a quite different way. Nevertheless, our crystalline specimens contain undegraded nucleic acid molecules in a nearly natural condition and the data should reflect some of the principal characteristics of their structure. A detailed analysis of the molecular structure of nucleic acid will require, in addition to the results presented here, a thorough examination of the diffraction spots obtainable from highly oriented specimens.

## SUMMARY

Aqueous systems of desoxyribonucleic acid (Na salt), over a range of concentrations from about 0.03 to 1.8 g/ml (2% to 100% by volume) have been submitted to X-ray diffraction analysis. The structure of the specimens is markedly dependent on the quantity of water present and on the method of preparation. Over a narrow concentration range, the material appears to be really crystalline and, on further dilution, the systems are paracrystalline over a wide range. A detailed analysis of the micellar structures is given for the paracrystalline specimens. These structures are more complex than in the case of tobacco mosaic virus, but also exhibit two-dimensional regularity and swell on dilution. The molecular fibre itself is rigid and has a diameter of about 16 Å. The most-favoured micelle consists of 7 molecules in a centred hexagonal arrangement. In the most ordered micellar systems, the structure possesses regularly disposed holes which produce an open honeycomb effect.

## RÉSUMÉ

Des systèmes aqueux d'acide desoxyribonucléique (sel de sodium), de concentrations comprises entre 0.03 et 1.8 g/ml (2% à 100% en volume) ont été soumis à l'analyse par diffraction des rayons-X. La structure du spécimen dépend considérablement de la quantité d'eau présente et de la méthode de préparation. Dans un domaine de concentration restreint la matière se montre réellement cristalline; lorsque la dilution augmente, les systèmes sont paracrystallins dans un large domaine. Les auteurs donnent une analyse détaillée des structures micellaires des spécimens paracrystallins. Ces structures sont plus complexes que dans le cas du virus de la mosaïque du tabac, mais elles montrent aussi une régularité à deux dimensions et elles gonflent à la dilution. La fibre moléculaire elle-même est rigide; son diamètre est de 16 Å environ. La micelle la plus favorisée consiste en 7 molécules en disposition hexagonale centrée. Les systèmes micellaires les plus ordonnés possèdent des trous disposés régulièrement qui produisent un effet de rayon de miel ouvert.

## ZUSAMMENFASSUNG

Wässrige Systeme von Desoxyribonukleinsäure (Natriumsalz), in einem Konzentrationsbereich von ungefähr 0.03 bis 1.8 g/ml (2 bis 100 Volumprozent) wurden der X-Strahlendiffraktions-Analyse unterworfen. Die Struktur der Proben ist deutlich abhängig von der Wassermenge und der Herstellungsmethode. In einem kleinen Konzentrationsbereich erscheint das Material wirklich kristallin; bei weiterer Verdünnung sind die Systeme in einem grossen Bereich parakristallin. Für die parakristallinen Proben wird eine ausführliche Analyse der Mizellenstrukturen dargelegt. Diese Strukturen sind komplexer als im Falle des Tabakmosaikvirus, aber sie zeigen auch eine zweidimensionale Regelmässigkeit und schwellen bei Verdünnung. Die molekulare Faser selbst ist steif und hat einen Durchmesser von ungefähr 16 Å. Die meist bevorzugte Mizelle besteht aus 7 Molekülen in hexogonaler zentrierter Anordnung. Die Struktur der regelmässigen Mizellensysteme enthält regelmässig angeordnete Löcher, welche an eine offene Honigwabe erinnern.

## REFERENCES

- <sup>1</sup> See, for example, A. L. DOUNCE, G. H. TISHKOFF AND S. R. FREER, *J. Gen. Physiol.*, 33 (1950) 629.
- <sup>2</sup> A. E. MIRSKY AND H. RIS, *J. Gen. Physiol.*, 31 (1947) 1.
- <sup>3a</sup> D. P. RILEY AND G. OSTER, *J. chim. phys.*, 47 (1950) 715.
- <sup>3b</sup> D. P. RILEY AND G. OSTER, *Trans. Faraday Soc.*, 46 (1950) 791.
- <sup>4</sup> R. SIGNER AND H. SCHWANDER, *Helv. Chim. Acta*, 32 (1949) 853.
- <sup>5</sup> J. A. V. BUTLER AND K. A. SMITH, *J. Chem. Soc.*, (1950) 3411.
- <sup>6</sup> G. OSTER, *J. chim. phys.*, 47 (1950) 717.
- <sup>7</sup> H. KÄHLER, *J. Phys. Colloid Chem.*, 52 (1948) 676.
- <sup>8</sup> R. CECIL AND A. G. OGSTON, *J. Chem. Soc.*, (1948) 1382.
- <sup>9</sup> H. L. NIXON AND G. OSTER, unpublished observations.
- <sup>10</sup> A. MÜLLER AND R. E. CLAY, *J. Inst. Elec. Engrs*, 84 (1939) 261.
- <sup>11a</sup> W. T. ASTBURY AND F. O. BELL, *Cold Spring Harbour Symposia Quant. Biol.*, 6 (1938) 109.
- <sup>11b</sup> W. T. ASTBURY AND F. O. BELL, *Nature*, 141 (1938) 747.
- <sup>12</sup> W. T. ASTBURY, *Symp. Soc. Exptl Biol.*, 12 (1947) 66.
- <sup>13</sup> G. OSTER AND D. P. RILEY, *Acta. Cryst.*, in press.
- <sup>14a</sup> G. OSTER AND D. P. RILEY, *Acta. Cryst.*, forthcoming.
- <sup>14b</sup> D. P. RILEY AND G. OSTER, *Trans. Faraday Soc.*, in press.
- <sup>15</sup> J. D. BERNAL AND I. FANKUCHEN, *J. Gen. Physiol.*, 25 (1941) 111.
- <sup>16</sup> G. OSTER, *J. Gen. Physiol.*, 33 (1950) 445.

Received June 18, 1951